Multi-wavelength imaging concepts for exoplanet detection

David Lafrenière*, René Doyon, René Racine, Christian Marois & Daniel Nadeau
Département de Physique, Université de Montréal, C.P. 6128, succ. Centre-ville
Montréal (Québec), Canada H3C 3J7

ABSTRACT

Direct exoplanet detections are currently limited by speckle noise arising from residual atmospheric wavefront errors and optical aberrations. Simultaneous spectral differential imaging (SSDI) is a high contrast imaging technique that aims at reducing this noise by the subtraction of images obtained simultaneously in adjacent narrow spectral bands. SSDI performances are severely degraded by differential optical aberrations between channels. We discuss two novel approaches to implement SSDI in which there are no differential aberrations. The first uses a microlens array at the focal plane to sample the point spread function (PSF) and micro-filters on the backside of each microlens to separate colors. The micropupils are immediately imaged on the detector. The second preserves the microlens array at the focal plane but re-images the array of micropupils through a beam-splitter on the detector. In both concepts the PSF measurement is made at the microlens array, so all optics is common prior to the PSF measurement in all colors. A simple prototype was used to test the concepts; preliminary results yield noise attenuation of $\sim 10^{-2}$.

Keywords: high contrast imaging, spectral differential imaging, speckle noise attenuation, exoplanets

1. INTRODUCTION

More than 100 exoplanets have been found by radial velocity surveys; the stage is now set for direct imaging. This is essential for subsequent determination of the properties of the planets from photometric measurements or spectroscopy. Direct imaging of exoplanets is a very challenging endeavor. They are hugely fainter, by a factor of 10^6 to 10^9, than their parent star and are located at very small angular separations. The planets are thus buried in the bright glare of the star even when observed with the best adaptive optics (AO) systems or with space telescopes. The detection limit of exoplanets is ultimately set by the photon noise of the central star's point spread function (PSF) but in practical setups there are far more important noises, in particular from speckles produced by residual atmospheric wavefront errors and by aberrated optics[1,2]. This "speckle noise" is by far the dominant noise component in current AO images; it must be somehow attenuated by a large factor.

Current high contrast imaging techniques involve either coronagraphy, PSF calibration, or both. Coronagraphy attenuates the coherent light of the on-axis PSF, thus reducing its photon noise, but hardly attenuates the speckle noise. As long as the latter constitutes the dominant source of noise, coronagraphy is only marginally beneficial. PSF calibration aims at subtracting the PSF structure and would ideally attenuate the speckle noise to the photon noise limit. The simplest calibration is the subtraction of the PSF of a reference star. However, PSF evolution caused by seeing variations, telescope and instrument flexures, primary mirror active control, slightly different optical paths or other quasi-static optical aberrations decorrelate the two PSFs and only modest attenuations can be achieved this way[3]. Roll deconvolution with HST is a slightly more sophisticated version of the same idea in which the telescope itself is rotated to obtain a reference PSF[4]. Again, telescope evolution (the so-called "breathing") decorrelates the PSFs and limits the attenuation. This underscores the difficulty of obtaining an accurate reference PSF.

Simultaneous spectral differential imaging (SSDI) is a calibration technique involving the simultaneous acquisition of images in adjacent narrow spectral bands in a spectral range where the stellar and planetary spectra differ appreciably[1,5-8]. Judicious image subtraction removes the stellar PSF and leaves that of any companion. At larger separations, the PSF scaling with wavelength allows this technique to be used to discriminate between a companion and a PSF structure even in the absence of differential spectral features. This is so because the PSFs must be re-scaled

* david@astro.umontreal.ca

before subtraction so the images of the companion do not overlay in the re-scaled images. SSDI does not suffer from the temporal evolution of the optics or atmosphere because the images are simultaneous, but its attenuation is hindered by differential aberrations between the spectral channels. The speckle noise attenuation is limited[3,9] to $N_{\Delta} / N \sim \sigma_{\Delta\phi}/\sigma_{\phi}$, where N_{Δ} is the noise in the difference, N the original PSF noise, σ_{ϕ} and $\sigma_{\Delta\phi}$ are the square root of the variance of the wavefront and wavefront difference respectively. Here, and in the rest of the paper, we quantify the PSF noise as the median over an annulus of the absolute value of the PSF image after subtraction of an azimuthally averaged profile. To achieve high ($<10^{-2}$) attenuations, it is crucial to minimize differential aberrations.

This paper discusses two possible implementations of SSDI in which there are no differential aberrations between the spectral bands because the spectral separation is made after the PSF measurement. Preliminary validation of the concept in the laboratory is also discussed. Integral field spectroscopy (IFS), if cautiously implemented, is another technique that would be efficient for SSDI but the concepts that we propose allow a much larger field of view, desirable for large scale surveys.

2. CONCEPT I: MULTI-COLOR DETECTOR ASSEMBLY (MCDA)

2.1. Concept

An MCDA[10,11] consists of the following. A checker board of four different narrowband micro-filters is deposited on the back side of a microlens array, each micro-filter being coincident with a microlens. The microlens array is then mounted over an infrared detector (Figure 1). When illuminated by a PSF of full-width at half-maximum (FWHM) equal to the spacing between at least four microlenses, the MCDA produces four well-sampled "checker board" images of the PSF, one in each color. Simple image processing can construct PSF images from these checker board images. An SSDI camera using an MCDA would thus only require simple optics to re-image the AO focal plane onto the microlens array at the proper scale.

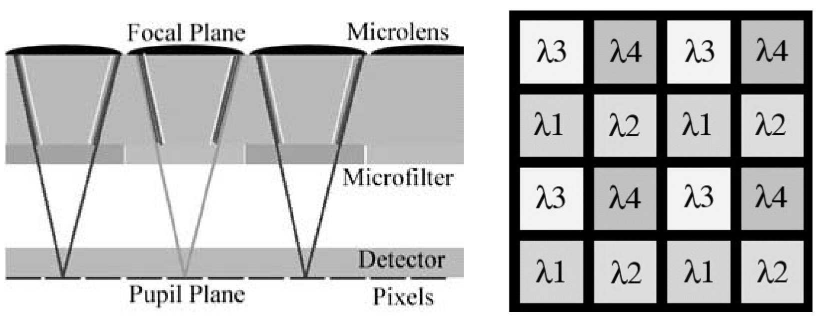

Figure 1: (left) cross-section view of an MCDA; (right) top view of an MCDA; λ1, λ2, λ3 and λ4 identify micro-filters of different colors.

2.2. Critical issues

The microlenses are used to concentrate the light of each PSF spatial sample onto well separated detector pixels to avoid spectral contamination of the signal caused by pixel cross-talk, which can be as high as ~6-15%[12]. PSFs of different wavelengths must be re-scaled prior to subtraction; thus, the leak of a sample to its neighbor in a different color will be carried to the wrong location in the PSF by the re-scaling and subtraction will leave residuals. For a spectral contamination of a factor X, the intensity of the residual will increase from 0 at the PSF center to X times the initial noise level at a separation where the shift introduced by the scaling is $\geq\lambda/D$. With current infrared detectors, it is possible to maintain the spectral contamination to less than 0.001 by using microlenses of f-ratios < 17 and separated by ~5 pixels. A mask on the microlens array could be used to block the light that may scatter at the microlenses interfaces.

If the transmittance of a microlens varies over its surface, then its mean transmittance is dependent on the illumination of the microlens. Since the illumination of the microlenses during a flat-field is different from the illumination during a target observation, the flat will not adequately correct for this effect. The same applies to the response of the pixels, which is non-uniform and thus dependent on the illumination of the pixel. However, these effects are local and fixed with respect to the microlens array and detector; if they are important, dithering between exposures can average the residuals. The residuals would also be on a scale smaller than the PSF and could be attenuated by proper filtering.

Refractive optics in the optical train prior to the MCDA and atmospheric differential refraction are potential sources of differential aberrations between the channels as they cause different wavelengths to go through slightly different paths through the optics. These effects can be mitigated by the use of an atmospheric dispersion corrector and reflective optics.

3. CONCEPT II: POST FOCAL PLANE ARRAY BEAM SPLITTER

3.1. Concept and layout

In an alternate implementation of the same concept that does not require the use of micro-filters, the focal plane is also sampled by a microlens array but the array of micro-pupils is then re-imaged through a beam splitter on the detector. The beam-splitter replicates the entire array of micro-pupils four times and a different narrowband filter is subsequently placed in each channel. This setup produces four images of the field in different colors. The layout is shown in Figure 2. In this concept, any optics following the microlens array only affect the micropupils. So as long as all the flux of each micropupil is recovered, the original AO PSF will be recovered in all colors regardless of differential optics below the microlens array. The considerations about flat-field and detector pixel response mentioned above also apply here.

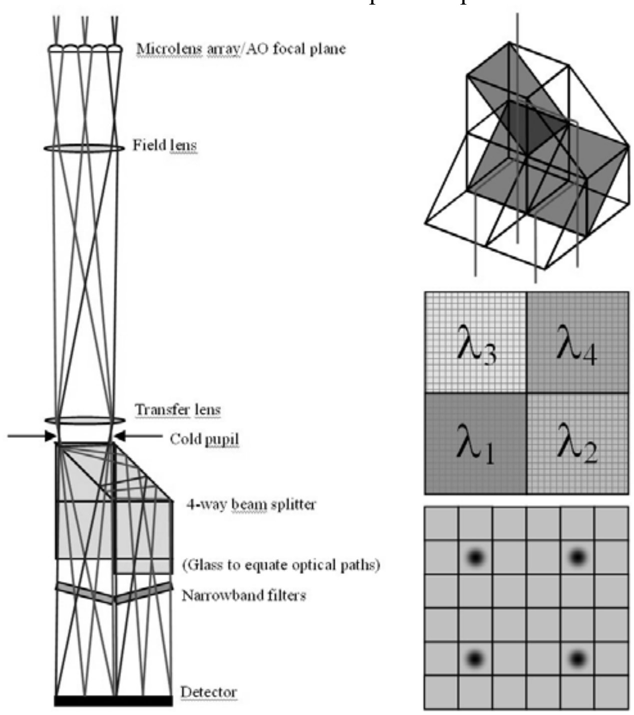

Figure 2: (left) schematic layout and ray traces of the concept; (top right) schematic of the four-way beam splitter using prisms, grey shading marks the splitting surfaces; (middle right) layout of the four colors on the detector; (bottom right) close-up showing the layout of micropupils on the detector.

3.2. Advantages

Besides avoiding the technical hurdles and cost of developing and fabricating micro-filters, this concept has other advantages over the MCDA. Since the same microlenses are used to sample the PSF in all colors, there is no need to over sample the PSF by a factor of two and the re-imaging optics can be made slower by a factor of two compared with the MCDA. Moreover, since neighboring samples are of the same color, the effect of sample cross-talk is less important because signal leaks cannot be carried over large distances by the re-scaling process. Also, similar signal leaks are present in all colors and are thus calibrated to first order by the subtraction. The reduced impact of sample cross-talk allows a smaller separation of micro-pupils on the detector and an increased field of view over an MCDA. A gain in throughput over the MCDA can be made by separating the beam using dichroics; this could provide a throughput as high as that of an IFS instrument with a much wider field of view.

4. MCDA TESTBED

4.1. Setup

For a first test of the concept, we purchased a stock microlens array of 200 µm pitch and f-ratio ~2.25 (at 1.6 µm) and mounted it over an engineering-grade Rockwell Hawaii-1 detector. The square microlens array is 10 mm on a side and covers one quadrant of the detector. Because of the short focal length of the microlenses, the microlens array was mounted with the curved surfaces towards the detector. A narrowband filter of bandwidth 1 % centered at 1.57 µm was used. No micro-filters were used. Simple refractive re-imaging optics were used to produce an ~f/800 beam reaching focus on the microlens array. This setup produces a PSF of FWHM equal to 6.3 microlenses on the microlens array. Microlens flat-field and microlens pinhole images were obtained (Figure 3), as well as flat-field images with the microlens array removed - the detector flat-field images. The micropupils have a FWHM of 0.8 pixel and are separated by 10.8 pixels on the detector.

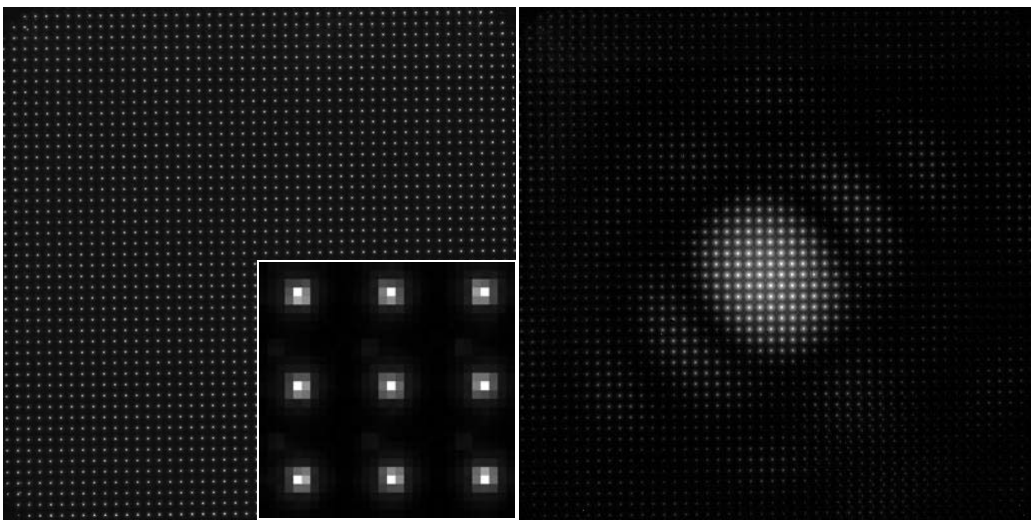

Figure 3: (left) microlens flat-field image, inset shows a close-up; (right) microlens pinhole image, logarithmic display.

4.2. Data reduction and results

Each image was dark subtracted and detector flat-fielded. The centroid of each micro-pupil was determined from the microlens flat-field image. A reduced flat-field was obtained by summing the signal of the microlens flat-field images in apertures of 2 pixel radius centered on each micro-pupil. The same summation was performed on the microlens pinhole images to obtain the PSF image. This image was then divided by the reduced flat-field image. Bad pixels were identified from the detector flat-field image and set to zero in every microlens image prior to summation of the signal in the apertures. Figure 4 shows the reduced PSF image.

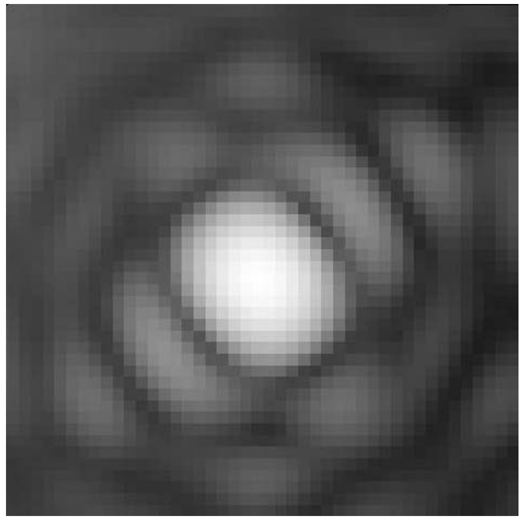

Figure 4: Reduced PSF image, logarithmic display, each pixel in this image corresponds to the signal of one micropupil integrated over an aperture of 2 pixel radius.

4.3. Noise attenuation

Three pixels out of four were made "blind" by multiplying the PSF image by a grid of 0 and 1. An interpolation over blind pixels was then made using the IDL function INTERPOLATE to obtain a first PSF image. The procedure was repeated to construct the three other PSFs by shifting the grid appropriately. The difference 0.5×[(PSF1+PSF4)-(PSF2+PSF3)] was then obtained. To reduce structures at spatial scales smaller than the PSF, the difference was convolved by a Gaussian of FWHM equal to that of the PSF. The residuals were then compared with the initial PSF noise convolved by the same Gaussian. The results are shown in Figure 5.

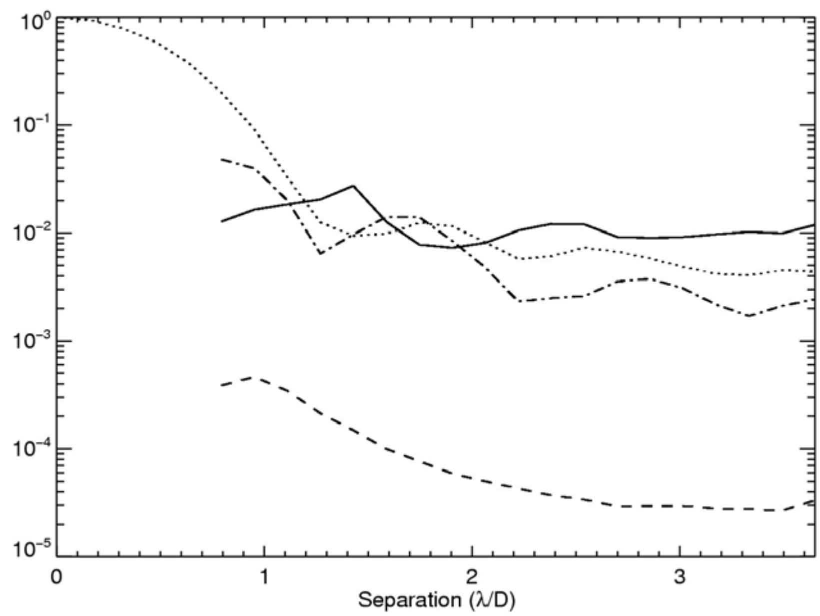

Figure 5: PSF noise attenuation. Original PSF intensity (dotted line), original PSF noise (dash-dot line), residual noise in convolved difference (dashed line) and noise attenuation factor (solid line). Noise calculations have been omitted in the PSF core region (< 5 pixel radius) because there are not enough pixels to obtain good statistics.

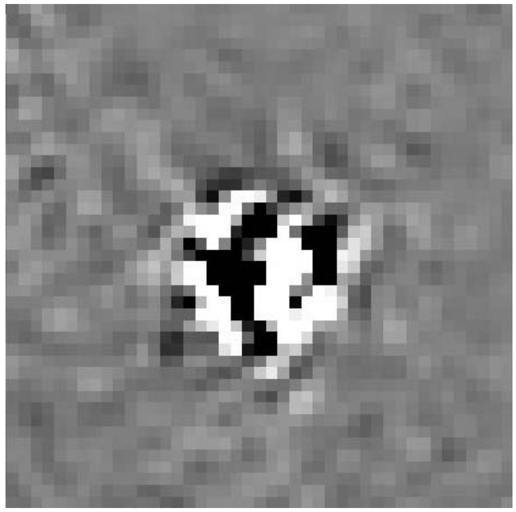

Figure 6: Difference image without convolution, each pixel in this image corresponds to the signal of one micropupil integrated over an aperture of 2 pixel radius. The display in the central region is saturated to show details at larger separations.

The residual image is pixelated (Figure 6); this indicates a good PSF structure subtraction but reveals the presence of a sample-to-sample noise in the original PSF. The residuals are more important than expected from photon noise or read noise and thus probably come from the flat-field. The exact cause of the residuals could not be determined and further experimentation is necessary.

These tests were performed in a single color. In a multi-color camera, chromatism of the PSF places a limit on the attenuation. The subtraction of two PSFs of different wavelengths can provide a maximum attenuation[3,9] of $N_\Delta /N \sim \Delta\lambda/\lambda$, where $\Delta\lambda$ and λ are the wavelength separation and mean wavelength of the two PSFs respectively. PSF calibrations using three and four wavelengths can provide attenuations of $\sim (\Delta\lambda/\lambda)^2$. Hence, using at least three narrowbands ($(\Delta\lambda/\lambda)^2 \sim 10^{-3}$), a multi-color camera should not suffer from chromatism if the sample cross-talk is well controlled.

5. ACKNOWLEDGEMENTS

This work was supported in part through grants from the Faculté des Études Supérieures de l'Université de Montréal, the Natural Sciences and Engineering Research Council, Canada and Fonds Québécois de la Recherche sur la Nature et les Technologies. The authors would like to thank Étienne Artigau for many helpful discussions and suggestions. Many thanks to Philippe Vallée and Jean-Sébastien Mayer for their help with the experimental setup.

REFERENCES

1. R. Racine, G. A. H. Walker, D. Nadeau, R. Doyon & C. Marois, *Speckle Noise and the Detection of Faint Companions*, PASP, 111, 587, 1999.
2. C. Marois, R. Doyon, R. Racine, & D. Nadeau, *Effects of Quasi-Static Aberrations in Faint Companion Searches*, EAS Publications Series 8, 233, 2003.
3. C. Marois, R. Doyon, D. Nadeau, R. Racine, M. Riopel & P. Vallée, *TRIDENT : an infrared differential imaging camera optimized for the detection of methanated substellar companions around nearby stars*, in preparation.
4. G. Schneider & M. D. Silverstone, Coronagraphy with HST: detectability is a sensitive issue, Proceedings SPIE 4860, 1, 2003.
5. W. H. Smith, *Spectral differential imaging detection of planets about nearby stars*, PASP, 99, 1344, 1987.
6. E. D. Rosenthal, M. A. Gurwell & P. T. P. Ho, *Efficient Detection of Brown Dwarfs Using Methane-Band Imaging*, Nature, 384, 243, 1996.

7. C. Marois, R. Doyon, R. Racine & D. Nadeau, *Efficient Speckle Noise Attenuation in Faint Companion Imaging*, PASP, 112, 91, 2000.
8. W. B. Sparks & H. C. Ford, *Imaging Spectroscopy for Extrasolar Planet Detection*, ApJ, 578, 543, 2002.
9. C. Marois, *La recherche de naines brunes et de planètes extrasolaires: développement d'une technique d'imagerie multi-bandes*, Ph. D. Thesis, 2004.
10. R. Doyon, D. Lafrenière, C. Marois, R. Racine & D. Nadeau, *Detecting and Characterizing Exo-planets using Multi-Color Detector Assemblies*, Proceedings SPIE "Second Workshop on Extremely Large Telescopes", in press.
11. C. Marois, R. Racine, R. Doyon, D. Lafrenière & D. Nadeau, *Differential Imaging with a Multi-Color Detector Assembly: A New ExoPlanet Finder Concept*, in preparation.
12. G. Finger, P. Biereichel, H. Mehrgan, M. Meyer, A. F. M. Moorwood, G. Nicolini & J. Stegmeier, *Infrared detector development programs for the VLT instruments at the European Southern Observatory*, Proceedings SPIE 3354, 87, 1998.